Extended Object Tracking Using Automotive Radar

Xiaomeng Cao **Jian Lan**

Center for Information Engineering
Science Research (CIESR),
School of Electronics and Information Engineering,
Xi'an Jiaotong University, Xi'an,
Shaanxi, 710049, P. R. China
xmcao911@163.com
lanjian@mail.xjtu.edu.cn

X. Rong Li

Department of
Electrical Engineering,
University of
New Orleans,
New Orleans,
LA 70148, U.S.A
xli@uno.edu

Yu Liu

ZOOX, Inc.
1149 Chess Dr,
Foster City,
CA 94404, U.S.A
yu@zoox.com

***Abstract*—For automotive radar-based extended object tracking (EOT), measurements are originated from the edges of the object, which usually has a regular shape. To handle this problem, this paper proposes an EOT approach, in which the object is assumed rectangular. Since a rectangular shape can be fully captured by its vertices, modeling and estimation of the extension can be reduced to those of the vertices, which are then included in the object state. Then an object being rectangular can be described as a quadratic equality constraint on the state. A measurement model is proposed with the scattering centers being assumed uniformly distributed over the observable edges of the object. It is further assumed that measurements at each time correspond to at most two adjacent boundary edges. By taking advantage of this, a data association method is proposed, in which the association events are largely eliminated. Given an association, the target state can be estimated in the linear minimum mean-square-error framework with the shape constraint treated as a pseudo-observation. The estimated state is then projected into the constraint space to improve estimation performance. Simulation results of an EOT scenario using automotive radar are given to illustrate the effectiveness of the proposed approach.**

I. Introduction

For self-driving vehicles, reliable environmental perception of their surroundings, including dynamic objects, is of utmost importance. To obtain an object-level representation of traffic participants so that safe maneuver planning can be provided, information of these objects' state, such as position and velocity, is needed.

By using classical target tracking techniques for point targets [1] [2], the kinematic state can be estimated easily based on the single measurement reflected from the object to be estimated. But by using high-resolution sensors (e.g., radar sensors, laser scanners, and stereo cameras) that self-driving cars are equipped with, multiple measurements from an object of a shape can be determined at each scan [3]. Thus, treating such an object as a point mass is no longer valid; we should consider it as an extended object. Using multiple measurements, not only the kinematic state but also the vehicle extension can be estimated. Moreover, in many applications, such as passing and parking, knowledge of extensions of surrounding vehicles is beneficial for safe maneuver planning. Therefore, the estimation of a vehicle should be considered as an extended object tracking (EOT) problem.

Here, we consider the problem of tracking an extended object based on automotive radars. For vehicle sensors, laser scanners usually can better infer the object extension than automotive radars in most cases, since laser scanners can acquire more reflected points from the target than radars. But this is not necessarily true in the following cases: (a) Automotive radars have more stable performance than laser scanners in complex weather conditions (e.g., rain, fog, and dust) and (b) Automotive radars outperform laser scanners for the extension of black targets or targets with mirrored surfaces, since the radar receives more reflected points from such objects than the scanner. Moreover, in the extreme case that the laser sensor is nonfunctional, the radar shall perceive the environment to make the vehicle's maneuver planning as safe as possible. Therefore, there is a pressing need for EOT using automotive radars.

Measurements made by automotive radars are around the object's physical boundary [4] [5]. This means that approaches and models proposed for EOT [6]–[10] (e.g., the random matrix approach [11]–[14]) in recent years are not suitable for tracking objects using automotive radars. The random matrix approach assumes that the measurements are uniformly distributed over the object extension [12]. In other existing approaches, including the random hypersurface model [15] [16] [17], measurements are assumed distributed over the target extension with specific models. These assumptions are largely invalid for automotive radars. Moreover, compared with laser scanners, automotive radars generate much fewer measurements with larger noise at each time. Thus, laser-sensor-based approaches, which track objects using their extension features extracted from many measurements in real time, may not provide a satisfactory estimation result for applications with automotive radars.

In recent years, several approaches [18] [5] have been proposed for EOT using automotive radars. In [18], only the kinematic state and the width of an object without other ex-

Research supported in part by grant for the National Natural Science Foundation of China (61573020) and NASA/LEQSF(2013-15)-Phase3-06 through grant NNX13AD29A.

978-0-9964527-7-9 ©2018 ISIF

tension parameters were estimated jointly. A direct scattering model was proposed in [5], where a vehicle was approximated by a rectangle with its length, width, and orientation estimated. However, the three parameters are not sufficient to characterize rectangles, since some other shapes, such as ellipses, also have these parameters. Thus, additional information must be incorporated to describe a rectangular shape, which makes the obtained model complicated. Since the scattering centers are not directly linear in these parameters, the measurement model could be highly nonlinear. In addition, all the existing tracking approaches ignore the constraint that the length and width are positive. Also, the proposed model in [5] may not be extended easily to track regular polygonal objects. In summary, a general and effective approach for tracking extended objects with regular polygonal shapes using automotive radars is still lacking.

In this paper, we propose a new model for a rectangular extension and an approach to EOT based on this model, since most vehicles are nearly rectangular. A rectangle can be fully determined by its four vertices. Thus, estimating a rectangular extension amounts to estimating its vertices, which are treated as the extension parameters.

As mentioned above, measurements from automotive radars originate from the object's physical boundary—the rectangle's four boundary edges. In this way, a measurement model for the four edges can be established based on the vertices. In the measurement model, a scattering center on an edge can be seen as a weighted sum of the two vertices of this edge. Compared with the previous model using the length, width, and orientation, the proposed model is much less nonlinear. For example, if the weights are given, the measurement model is linear in the state of the vehicle. In fact, the detected points are from at most two adjacent boundary edges of the vehicle with respect to the aspect angle under which the radar sees the vehicle. As the relative position and orientation between the radar and the object may change over time, the measurement configuration —one or both adjacent edges that generate the measurements—may change accordingly. Thus, we consider determining the configuration using the maximum likelihood (ML) method first, so the association can be eliminated, largely reducing the algorithm complexity. Then we use the probabilistic data association (PDA) with a gating method to associate the measurements with the two edges in the determined configuration. By taking advantage of this, estimation performance can be largely improved.

For regular polygons, regularity means that all the inner angles are known a priori. For example, the two adjacent boundary edges of a rectangle are perpendicular to each other. This information can be expressed by the constraint on the vertices. Actually, the constraint is a piece of prior information about the object extension. Existing EOT approaches ignore this prior constraint information, which, however, should be incorporated into EOT to improve estimation. In view of this and based on the proposed model, we provide an EOT approach considering prior constraint information. This prior information can be described as a nonlinear equality constraint on the state, and the pseudo-observation and projection methods are used to solve the constrained estimation problem. The effectiveness of what is proposed is demonstrated by several illustrative simulations.

This paper is organized as follows. Section II proposes a new model to describe the rectangular extension of an object and an approach for EOT based on this new model. Section III presents simulation results to demonstrate the effectiveness of the proposed approach. Section IV concludes the paper.

II. Extended Object Tracking Based on Automotive Radar measurements

A. System Models

Consider the following system models:

$$x_k = h(x_{k-1}, w_{k-1}) \tag{1}$$

$$z_k^r = g(x_k, v_k^r),\ r = 1, ..., N_k \tag{2}$$

They describe the target dynamics and sensor measurements, where x_k is the state vector with transition function h, z_k^r is one of a total of N_k measurements of the extended object with the measurement function g, k is the time index, and $w_k \sim N(0, Q_k)$ and $v_k \sim N(0, R_k)$ are independent Gaussian noise.

Unlike a point target, for EOT, the state vector $x_k = [(x_k^c)^{\mathrm{T}}, (x_k^s)^{\mathrm{T}}]^{\mathrm{T}}$ to be estimated at time k includes a random vector x_k^c representing the centroid state of the object and a random vector x_k^s characterizing the extension. Consider $x_k^c = [\mathrm{x}_k, \dot{\mathrm{x}}_k, \mathrm{y}_k, \dot{\mathrm{y}}_k]^{\mathrm{T}}$, where $x_k^{cp} = (\mathrm{x}_k, \mathrm{y}_k)^{\mathrm{T}}$ and $(\dot{\mathrm{x}}_k, \dot{\mathrm{y}}_k)$ are the position and velocity of the target in the Cartesian plane, respectively.

Let $Z_k = \{z_k^r\}_{r=1}^{N_k}$ denote the set of N_k measurements at time k. As z_k^r is a noisy version of the noiseless measurement z_k^{r*} on the extended object [12] [15], the measurement equation (2) can be rewritten as

$$z_k^r = z_k^{r*} + v_k^r. \tag{3}$$

B. A New Model Using Automotive Radar Measurements

In our method for vehicle tracking, the extension of the extended object is modeled by a rectangle. A rectangle is fully characterized by its four vertices, as shown in Fig. 1, where $\{p_k^i\}_{i=1}^4$ denote the relative positions of the four vertices to the centroid position $O \triangleq x_k^{cp}$. Thus, we can treat these relative positions as the extension parameters to be estimated. Clearly,

$$p_k^3 = -p_k^1,\ p_k^4 = -p_k^2 \tag{4}$$

That is, obtaining p_k^1 and p_k^2 is enough to represent the rectangle. In this way, the extension parameter vector x_k^s is reduced to

$$x_k^s = [(p_k^1)^{\mathrm{T}}, (p_k^2)^{\mathrm{T}}]^{\mathrm{T}} \tag{5}$$

As the extension is a rectangle, we have

$$\vec{Op_k^{1,2}} \perp \vec{p_k^1 p_k^2}, \tag{6}$$

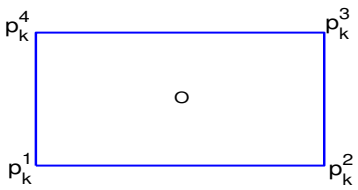

Figure 1: Representing a vehicle by a rectangle

where $p_k^{1,2} = \frac{1}{2}(p_k^1 + p_k^2)$, $\overrightarrow{Op_k^{1,2}}$ is the vector from O to $p_k^{1,2}$, and $\overrightarrow{p_k^1 p_k^2}$ is the vector from p_k^1 to p_k^2. Equation (6) can be rewritten as

$$(p_k^1 + p_k^2)^{\mathrm{T}}(p_k^1 - p_k^2) = 0 \tag{7}$$

Then we can easily get

$$([0_{2\times4}, I_2, I_2]x_k)^{\mathrm{T}}([0_{2\times4}, I_2, -I_2]x_k) = 0, \tag{8}$$

where $0_{2\times4}$ denotes the 2×4 zero matrix and I_2 is the 2×2 identity matrix. Thus, the constraint on the state becomes

$$x_k{}^{\mathrm{T}} D x_k = 0, \tag{9}$$

where $D = [0_{2\times4}, I_2, I_2]^{\mathrm{T}}[0_{2\times4}, I_2, -I_2] = \begin{bmatrix} 0_{4\times4} & 0_{4\times4} \\ 0_{4\times4} & \tilde{D} \end{bmatrix}$ and $\tilde{D} = \begin{bmatrix} I_2 & -I_2 \\ I_2 & -I_2 \end{bmatrix}$.

As mentioned above, the detected points of automotive radars are located on the physical boundary of the object. Since the target is a rectangle, the noiseless measurements are supposed to be located on its four edges. Denote $p_k^i p_k^{i+1}$ as the boundary edge between p_k^i and p_k^{i+1} ($p_k^5 \triangleq p_k^1$ and $p_k^6 \triangleq p_k^2$). The measurement z_k^r from each edge can be given as

$$z_k^r = \begin{cases} s_k^r p_k^1 + (1 - s_k^r)p_k^2 + x_k^{cp} + v_k^r, \text{ if } z_k^r \text{ is from } p_k^1 p_k^2 \\ s_k^r p_k^2 + (1 - s_k^r)p_k^3 + x_k^{cp} + v_k^r, \text{ if } z_k^r \text{ is from } p_k^2 p_k^3 \\ s_k^r p_k^3 + (1 - s_k^r)p_k^4 + x_k^{cp} + v_k^r, \text{ if } z_k^r \text{ is from } p_k^3 p_k^4 \\ s_k^r p_k^4 + (1 - s_k^r)p_k^1 + x_k^{cp} + v_k^r, \text{ if } z_k^r \text{ is from } p_k^4 p_k^1 \end{cases} \tag{10}$$

where $0 \le s_k^r \le 1$. If many measurements are given, their specific distribution on the boundary edge can be learned, as the approach proposed in [19]. Without further information, s_k can be assumed uniformly distributed over $[0, 1]$ a priori. From equation (4), it follows that (10) becomes

$$z_k^r = \begin{cases} s_k^r p_k^1 + (1 - s_k^r)p_k^2 + x_k^{cp} + v_k^r, \text{ if } l_k^1 \\ s_k^r p_k^2 - (1 - s_k^r)p_k^1 + x_k^{cp} + v_k^r, \text{ if } l_k^2 \\ -s_k^r p_k^1 - (1 - s_k^r)p_k^2 + x_k^{cp} + v_k^r, \text{ if } l_k^3 \\ -s_k^r p_k^2 + (1 - s_k^r)p_k^1 + x_k^{cp} + v_k^r, \text{ if } l_k^4 \end{cases} \tag{11}$$

where l_k^i denotes the event that z_k^r is from the edge $p_k^i p_k^{i+1}$. Thus, we have

$$z_k^r = \tilde{g}_{i(r)}(x_k, s_k^r, v_k^r) = H_i x_k + v_k^r, \text{ if } l_k^i \tag{12}$$

where $i = 1, ..., 4$,

$$H_1 = [B,\ s_k^r I_2,\ (1 - s_k^r)I_2]$$
$$H_2 = [B,\ (s_k^r - 1)I_2,\ s_k^r I_2]$$
$$H_3 = [B,\ -s_k^r I_2,\ (s_k^r - 1)I_2]$$
$$H_4 = [B,\ (1 - s_k^r)I_2,\ -s_k^r I_2]$$

and $B = \begin{bmatrix} 1 & 0 & 0 & 0 \\ 0 & 0 & 1 & 0 \end{bmatrix}$. In this way, the measurement model for all four edges is obtained.

Remark 1: (a) A novel model for describing a rectangular object is proposed. In this model, the estimation of the object extension is reduced to that of its vertices, which are treated as components of the extension state.

(b) The shape of a rectangle entails a quadratic equality constraint on the state. The constraint represents prior information about the object extension, and should be used in EOT for better estimation. How to use this information in estimation is given later.

(c) The measurement model is proposed with the noiseless measurements being assumed uniformly distributed over the observable edges of the object extension. It naturally connects the measurements and the vertices, which is also suitable for describing other polygons.

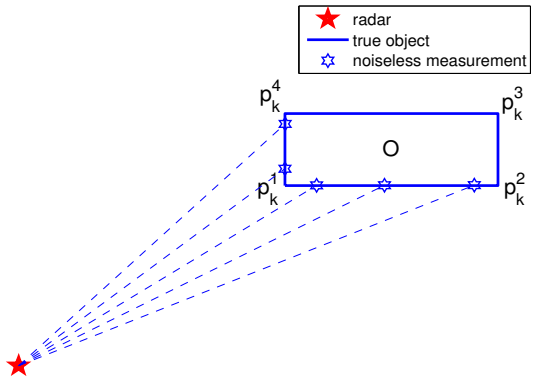

Figure 2: The configuration of measurements on the edges of the target extension

C. Data Association

In fact, although the measurements originate from the edges of the object extension, the exact edge that generates the measurement z_k^r is unknown. Generally, all association possibilities must be considered, which can be quite complicated in practice.

Therefore, we consider simplifying the data association by utilizing special features of rectangles. For such a shape, the detected points are from at most two adjacent edges of the vehicle, as shown in Fig. 2. Thus, on the edges of a rectangle, there are four measurement configurations, L_k^i $(i = 1, ..., 4)$: the measurements at time k are from edges $p_k^i p_k^{i+1}$ and $p_k^{i+1} p_k^{i+2}$. In particular, the situation that the measurements are only from one edge, $p_k^i p_k^{i+1}$ or $p_k^{i+1} p_k^{i+2}$, is a special case of L_k^i. At each time k, the true measurement-configuration is denoted as L_k^t, $t \in \{1,\ 2,\ 3,\ 4\}$ and may change over time depending on the relative position and orientation between the radar and the vehicle.

The determination of the configuration for Z_k is much easier than that of the edge generating each measurement z_k. Once the configuration is given, the association events can be largely eliminated. Thus, we consider determining the configuration first using an ML method. Then, we use the PDA method to associate the measurements with the edges in the determined configuration. The details are as follows.

1) Configuration Determination by MLE: The configuration L_k^t is determined as

$$\hat{t} \triangleq \arg \max_{t \in \{1,\,2,\,3,\,4\}} \mathrm{L}(L_k^t | Z^k) \tag{13}$$

where $Z^k = (Z_1, ..., Z_{k-1}, Z_k)$, $\hat{t}$ is the estimate of t and

$$\begin{aligned}
\mathrm{L}(L_k^t|Z^k) &\triangleq p(Z_k|L_k^t, Z^{k-1}) \\
&= \prod_{r=1}^{N_k} p(z_k^r|L_k^t, Z^{k-1}) \\
&= \prod_{r=1}^{N_k} [p(z_k^r, l_k^t|L_k^t, Z^{k-1}) + p(z_k^r, l_k^{t+1}|L_k^t, Z^{k-1})] \\
&= \prod_{r=1}^{N_k} [p(z_k^r|l_k^t, Z^{k-1}) P\{l_k^t|L_k^t, Z^{k-1}\} \\
&\quad + p(z_k^r|l_k^{t+1}, Z^{k-1}) P\{l_k^{t+1}|L_k^t, Z^{k-1}\}]
\end{aligned} \tag{14}$$

where l_k^i denotes the event that z_k^r is from the edge $p_k^i p_k^{i+1}$. For the event L_k^t, without further information, the probabilities of l_k^t and l_k^{t+1} conditioned on L_k^t and Z^{k-1} are assumed both to be $1/2$.

To calculate $p(z_k^r|l_k^t, Z^{k-1})$, we assume that conditioned on l_k^t and Z^{k-1} measurement z_k is Gaussian distributed:

$$p(z_k|l_k^t, Z^{k-1}) = N(z_k; \check{z}_k^t, P_{z_k}^t) \tag{15}$$

where

$$\check{z}_k^t \triangleq E(z_k|l_k^t, Z^{k-1}) \tag{16}$$

$$P_{z_k}^t \triangleq E(\left[z_k - \check{z}_k^t\right]\left[z_k - \check{z}_k^t\right]^{\mathrm{T}} | l_k^t, Z^{k-1}) \tag{17}$$

They are obtained based on the state prediction and equation (12) by the unscented transformation (UT) and $s_k \sim U(0,1)$. Details of the calculation are given in (b) of Subsection II.E.

2) Probabilistic Data Association: Here, we associate the measurements with the two determined edges $\hat{p}_{k|k-1}^{\hat{t}}\hat{p}_{k|k-1}^{\hat{t}+1}$ and $\hat{p}_{k|k-1}^{\hat{t}+1}\hat{p}_{k|k-1}^{\hat{t}+2}$ [20].

$$\begin{aligned}
\hat{x}_{k|k} &= \sum_{e=1}^{m_k} E\left[x_k|\varphi_k^e, Z^k\right] P\left\{\varphi_k^e|Z^k\right\} \\
&= \frac{1}{c}\sum_{e=1}^{m_k} \bar{x}_{k|k}^e \Lambda_k^e P\left\{\varphi_k^e|Z^{k-1}\right\}
\end{aligned} \tag{18}$$

$$\begin{aligned}
P_{k|k} &= MSE(\hat{x}_{k|k}) \\
&= \frac{1}{c}\sum_{e=1}^{m_k} \Lambda_k^e P\left\{\varphi_k^e|Z^{k-1}\right\} (\bar{P}_{k|k}^e + [\bar{x}_{k|k}^e - \hat{x}_{k|k}] \\
&\quad \times [\bar{x}_{k|k}^e - \hat{x}_{k|k}]^{\mathrm{T}})
\end{aligned} \tag{19}$$

where φ_k^e, $e = 1, ..., m_k$, denotes the association event, $\bar{x}_{k|k}^e \triangleq E\left[x_k|\varphi_k^e, Z^k\right]$ and $\bar{P}_{k|k}^e$ are the state estimate at time k under φ_k^e and its MSE matrix, respectively, $\hat{x}_{k|k}$ and $P_{k|k}$ are the state estimate at time k and its mean-square error (MSE) matrix, respectively. To associate N_k measurements with two edges, there are $m_k = (2)^{N_k}$ possibilities. $P\left\{\varphi_k^e|Z^k\right\}$ is the association probability at time k, and

$$\Lambda_k^e = p(Z_k|\varphi_k^e, Z^{k-1}) \tag{20}$$

$$c = \sum_{e=1}^{m_k} \Lambda_k^e P\left\{\varphi_k^e|Z^{k-1}\right\} \tag{21}$$

Without further information, we assume

$$P\left\{\varphi_k^e|Z^{k-1}\right\} = 1/m_k, e = 1, ..., m_k$$

To calculate Λ_k^e, Z_k conditioned on (φ_k^e, Z^{k-1}) is assumed to be Gaussian distributed.

The number m_k of association events can be very large depending on the number of measurements at time k. Considering all the association events in the PDA method will make the algorithm very complex. Therefore, we use gating to reduce m_k as follows.

We set a gate for each of the two determined edges:

$$\nu_k^1 = \{z_k : [z_k - \check{z}_k^{\hat{t}}]^{\mathrm{T}} (P_{z_k}^{\hat{t}})^{-1} [z_k - \check{z}_k^{\hat{t}}] \le \gamma \tag{22}$$

$$\nu_k^2 = \{z_k : [z_k - \check{z}_k^{\hat{t}+1}]^{\mathrm{T}} (P_{z_k}^{\hat{t}+1})^{-1} [z_k - \check{z}_k^{\hat{t}+1}] \le \gamma \tag{23}$$

where ν_k^1 and ν_k^2 represent the two elliptical gates, γ is the gate threshold determined by the gating probability [20]. These two gates are illustrated in Fig. 3 for $\hat{t} = 4$.

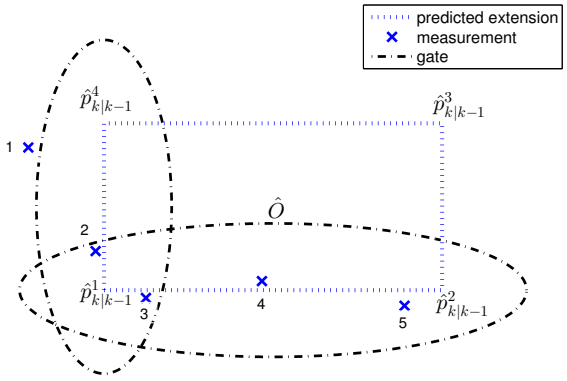

Figure 3: Gates

A measurement inside a single gate is regarded as generated from the corresponding edge. Then we consider all the possibilities to associate the remaining measurements with the two determined edges.

Take Fig. 3 for example. We can see that the measurements '4' and '5' are inside the horizontal elliptical gate only. So these two measurements are deemed from the edge $\hat{p}_{k|k-1}^1\hat{p}_{k|k-1}^2$. Then we only associate the other three measurements, '1', '2', and '3' ('1' is outside both gates) with the two determined edges. In this way, the number of association events can be reduced largely and the algorithm complexity

can be decreased. The number of association events for the remaining measurements is denoted as $\breve{m}_k$.

Remark 2: We provide the likelihood function of an edge under a Gaussian assumption. In this way, both the likelihood and the gates can be easily obtained.

D. Constrained Estimation

Here, we consider the state estimation with constraints, since the extension to be estimated is a rectangle and there is a constraint on the state, according to equation (9).

Many approaches have been proposed for state estimation with constraints. They include the reparameterization [21] [22], pseudo-observation [23] [24], projection [25] [26], and others. The reparameterization method reparameterizes the system so that the equality constraint can be satisfied naturally. It is, however, not suitable for systems with nonlinear constraints, such as our constraint in equation (9). So in this paper, we consider using pseudo-observation and projection methods.

To obtain $\bar{x}^e_{k|k} \triangleq E\left[x_k|\varphi^e_k, Z^k\right]$ in equation (18), the pseudo-observation method is augmented by the measurement set with the pseudo-measurement 0 of ${x_k}^{\mathrm{T}} D x_k$. By equation (12), we have

$$\begin{aligned}\begin{bmatrix} z_k^1 \\ \vdots \\ z_k^{N_k} \\ 0 \end{bmatrix} &= \begin{bmatrix} \begin{bmatrix} \tilde{g}^e_{i(1)}(x_k, s_k^1, v_k^1) \\ \vdots \\ \tilde{g}^e_{i(N_k)}(x_k, s_k^{N_k}, v_k^{N_k}) \end{bmatrix} \\ {x_k}^{\mathrm{T}} D x_k \end{bmatrix} \\ &= \breve{g}^e(x_k, s_k^1, ...s_k^{N_k}, v_k^1, ..., v_k^{N_k}) \end{aligned} \tag{24}$$

where $\tilde{g}^e_{i(r)}$, $r = 1, ..., N_k$, is the measurement model for z_k^r under φ^e_k. The measurement model for $i = 1, ..., 4$ is given by equation (12). $\breve{g}^e$ denotes the overall function under φ^e_k.

In fact, since $\breve{g}^e$ is nonlinear in x_k, it is not easy to obtain $\bar{x}^e_{k|k}$. Therefore, we use the linear minimum mean-square error (LMMSE) estimation framework to estimate x_k under φ^e_k. The estimate and the corresponding MSE matrix are denoted as $\hat{x}^e_{k|k}$ and $P^e_{k|k}$, respectively, to be given in the next subsection. The moments related to the measurements augmented by the pseudo-observation are calculated by UT.

Equation (24) is nonlinear. The estimate $\hat{x}^e_{k|k}$ does not necessarily satisfy it. That is, the estimated extension under φ^e_k is not necessarily a rectangle: ${\hat{x}^e_{k|k}}^{\mathrm{T}} D \hat{x}^e_{k|k} \neq 0$. Thus, we project $\hat{x}^e_{k|k}$ into the constraint space, so the result strictly satisfies the constraint:

$$\hat{x}^{e,p}_{k|k} = \arg\min_y (y - \hat{x}^e_{k|k})^{\mathrm{T}} W_k (y - \hat{x}^e_{k|k}) \tag{25}$$

$$s.t.\ y^{\mathrm{T}} D y = 0 \tag{26}$$

where $\hat{x}^{e,p}_{k|k}$ is the projected result of $\hat{x}^e_{k|k}$, W_k is a positive definite weighting matrix, chosen as $(P^e_{k|k})^{-1}$.

Since the constraint is nonlinear in the state, we linearize it around $\hat{x}^e_{k|k}$ in a first-order Taylor series:

$$y^{\mathrm{T}} D y \approx (\hat{x}^e_{k|k})^{\mathrm{T}} D \hat{x}^e_{k|k} + (2D\hat{x}^e_{k|k})^{\mathrm{T}} (y - \hat{x}^e_{k|k}) \tag{27}$$

Then, constraint (26) can be approximated as

$$(\hat{x}^e_{k|k})^{\mathrm{T}} D \hat{x}^e_{k|k} + (2D\hat{x}^e_{k|k})^{\mathrm{T}} (y - \hat{x}^e_{k|k}) = 0 \tag{28}$$

Thus, $\hat{x}^{e,p}_{k|k}$ can be obtained easily [21]:

$$\begin{aligned}\hat{x}^{e,p}_{k|k} = \hat{x}^e_{k|k} &+ P^e_{k|k}(2D\hat{x}^e_{k|k})[(2D\hat{x}^e_{k|k})^{\mathrm{T}} P^e_{k|k} \\ &\times (2D\hat{x}^e_{k|k})]^{-1}[(2D\hat{x}^e_{k|k})^{\mathrm{T}} \hat{x}^e_{k|k} \\ &- (\hat{x}^e_{k|k})^{\mathrm{T}} D \hat{x}^e_{k|k} - (2D\hat{x}^e_{k|k})^{\mathrm{T}} \hat{x}^e_{k|k}] \end{aligned} \tag{29}$$

$$P^{e,p}_{k|k} = A_e P^e_{k|k} A_e^{\mathrm{T}} \tag{30}$$

where

$$\begin{aligned} A_e = I - P^e_{k|k}(2D\hat{x}^e_{k|k})[(2D\hat{x}^e_{k|k})^{\mathrm{T}} P^e_{k|k} \\ \times (2D\hat{x}^e_{k|k})]^{-1}(2D\hat{x}^e_{k|k})^{\mathrm{T}} \end{aligned} \tag{31}$$

Finally, the overall estimate $\hat{x}_{k|k}$ is a probabilistically weighted sum of the projected estimates $\left\{\hat{x}^{e,p}_{k|k}\right\}_{e=1}^{\breve{m}_k}$.

E. Algorithm

Here is one cycle of the proposed approach (given $\hat{x}_{k-1|k-1}$, $P_{k-1|k-1}$).

(a) *State Prediction:* Obtain the prediction $\hat{x}_{k|k-1}$ and covariance $P_{k|k-1}$ based on the dynamic system (1). For a linear system given by

$$x_k = F_k x_{k-1} + G_k w_{k-1} \tag{32}$$

they can be calculated exactly as in the Kalman filter:

$$\hat{x}_{k|k-1} = F_k \hat{x}_{k-1|k-1} \tag{33}$$

$$P_{k|k-1} = F_k P_{k-1|k-1} F_k^{\mathrm{T}} + G_k Q_{k-1} G_k^{\mathrm{T}} \tag{34}$$

(b) *UT:* Based on equation (12) and the state prediction, obtain the mean $\check{z}^t_k$ and the covariance $P^t_{z_k}$ in equations (16) and (17) of the measurements from the edge $\hat{p}^t_{k|k-1}\hat{p}^{t+1}_{k|k-1}$ by using UT, where $\hat{p}^1_{k|k-1}, ..., \hat{p}^4_{k|k-1}$ are the vertices of the predicted rectangular extension.

Since s_k and v_k in equation (12) are unknown, we augment the state vector as

$$x^a_k \triangleq \left[(x_k)^{\mathrm{T}}, s_k,\ v_k\right]^{\mathrm{T}} \tag{35}$$

where $s_k \sim U(0, 1)$, and $v_k \sim N(0, R_k)$. Note that the state to be estimated in this paper is x_k. It is augmented here just to calculate the moments related to the measurements. The state augmentation in Section II.E(d) is for the same purpose.

UT approximates the mean and covariance of a nonlinear function d of a random vector x by deterministic sample points $\left\{d(x^j)\right\}$ with weights $\{\alpha_j\}_{j=1}^{\tilde{N}}$.

$$(\bar{d}, P_d) = \ \mathrm{UT}[d(x), \bar{x}, P_x] \tag{36}$$

where $\bar{x}$ and P_x are the mean and covariance of x, respectively,

$$\bar{d} = \sum_{j=1}^{\tilde{N}} \alpha_j d(x^j) \tag{37}$$

$$P_d = \sum_{j=1}^{\tilde{N}} \alpha_j (d(x^j) - \bar{d})(d(x^j) - \bar{d})^{\mathrm{T}} \tag{38}$$

Then, we have

$$\begin{aligned}(\check{z}_k^t, P_{z_k}^t) &= \mathrm{UT}[\tilde{g}_t(x_k^a), \hat{x}_{k|k-1}^a, P_{k|k-1}^a] \\ &= \mathrm{UT}[\tilde{g}_t(x_k, s_k, v_k), [(\hat{x}_{k|k-1})^{\mathrm{T}}, \bar{s}_k, 0]^{\mathrm{T}}, \\ &\quad \mathrm{diag}\left(P_{k|k-1}, C_{s_k}, R_k\right)] \end{aligned} \tag{39}$$

where $\bar{s}_k$ and C_{s_k} are the mean and covariance of s_k, respectively.

(c) *Data Association:* By equations (13) and (14), obtain the configuration $L_k^{\hat{t}}$ as

$$\begin{aligned}\hat{t} &\triangleq \arg \max_{t \in \{1,\,2,\,3,\,4\}} \mathrm{L}(L_k^t | Z^k) \\ &= \arg \max_{t \in \{1,\,2,\,3,\,4\}} \prod_{r=1}^{N_k} [N(z_k^r; \check{z}_k^t, P_{z_k}^t) + N(z_k^r; \check{z}_k^{t+1}, P_{z_k}^{t+1})] \end{aligned} \tag{40}$$

Draw two gates ν_k^1 and ν_k^2 according to equations (22) and (23). A measurement inside a single gate is treated as from the corresponding edge. Then associate the rest measurements with the two determined edges.

(d) *Measurement Prediction:* The measurement set Z_k is augmented with the pseudo-measurement 0 of ${x_k}^{\mathrm{T}} D x_k$: $Z_k^A = [Z_k^{\mathrm{T}}, 0]^{\mathrm{T}}$. The state vector is augmented to calculate the measurement prediction $\hat{Z}_{k|k-1}^{A,e}$ and covariance S_k^e:

$$x_k^A \triangleq \left[x_k^{\mathrm{T}}, s_k^1, ..., s_k^{N_k}, v_k^1, ..., v_k^{N_k}\right]^{\mathrm{T}} \tag{41}$$

Then we have

$$\begin{aligned}(\hat{Z}_{k|k-1}^{A,e}, S_k^e) &= \mathrm{UT}[\breve{g}^e(x_k^A), (\hat{x}_{k|k-1}^A)^{\mathrm{T}}, P_{k|k-1}^A] \\ &= \mathrm{UT}[\breve{g}^e(x_k, s_k^1, ...s_k^{N_k}, v_k^1, ..., v_k^{N_k}), \\ &\quad [\hat{x}_{k|k-1}^{\mathrm{T}}, \bar{s}_k^1, ..., \bar{s}_k^{N_k}, \bar{v}_k^1, ..., \bar{v}_k^{N_k}]^{\mathrm{T}}, \\ &\quad \mathrm{diag}(P_{k|k-1}, C_{s_k}, ..., C_{s_k}, R_k, ..., R_k)] \end{aligned} \tag{42}$$

$$C_{xz}^e = \sum_{j=1}^{\tilde{N}} a_j (x_k^j - \hat{x}_{k|k-1})(\breve{g}^e(x_k^{A,j}) - \hat{Z}_{k|k-1}^{A,e})^{\mathrm{T}} \tag{43}$$

where $\breve{g}^e$ is the function under φ_k^e, defined in equation (24), and x_k^j and $x_k^{A,j}$ are the sample points of x_k and x_k^A, respectively.

(e) *Update:*

$$K_k^e = C_{xz}^e (S_k^e)^{-1} \tag{44}$$

$$\hat{x}_{k|k}^e = \hat{x}_{k|k-1} + K_k^e (Z_k^A - \hat{Z}_{k|k-1}^{A,e}) \tag{45}$$

$$P_{k|k}^e = P_{k|k-1} - K_k^e S_k^e (K_k^e)^{\mathrm{T}} \tag{46}$$

(f) *Projection:* $\hat{x}_{k|k}^{e,p}$ and $P_{k|k}^{e,p}$ are given in equations (29)–(31).

(g) *Overall Estimation:* The overall estimation is given by equations (18)–(19), where $\Lambda_k^e = N(Z_k^A; \hat{Z}_{k|k-1}^{A,e}, S_k^e)$, and $\bar{x}_{k|k}^e$ and $\bar{P}_{k|k}^e$ are replaced with $\hat{x}_{k|k}^{e,p}$ and $P_{k|k}^{e,p}$, respectively.

Remark 3: (a) In the estimation, treating s_k as a random variable uniformly distributed over $[0, 1]$ is beneficial. Although we can associate these measurements with the edges of the rectangular extension, the exact positions from which the measurements come are still unknown. Without further information, the measurements can be assumed uniformly distributed over an edge, which means that s_k is uniformly distributed over $[0, 1]$. In fact, the effect of s_k can be handled simply and systematically, as stated next.

(b) Using the LMMSE estimation can systematically solve the problems caused by the shape constraint and the random variable s_k. LMMSE estimators can handle the shape constraint directly as part of the measurements. The parameter s_k affects the estimation result only through the moments related to the measurements, which can be calculated by deterministic sampling (e.g., UT).

Remark 4: The proposed approach has the following merits. (a) It takes advantage of the special features of the problem of tracking a rectangular object to eliminate the association events, so the algorithm complexity is reduced significantly. (b) The idea of introducing, modeling, and application of the shape constraints can be extended to EOT with polygon shapes.

III. Simulation Results

To illustrate the effectiveness of our proposed approach, simulation examples are provided in this section. Consider a scenario in which an extended object moves at a nearly constant-velocity (CV) in the x-y plane [27]. The following was used:

$$\begin{aligned} x_k &= [(x_k^c)^{\mathrm{T}}, (x_k^s)^{\mathrm{T}}]^{\mathrm{T}} \\ x_k^c &= [x_k^{cp_x}, x_k^{cv_x}, x_k^{cp_y}, x_k^{cv_y}]^{\mathrm{T}} \\ x_k^s &= [(p_k^1)^{\mathrm{T}}, (p_k^2)^{\mathrm{T}}]^{\mathrm{T}} \end{aligned}$$

$$F_k = \mathrm{diag}(F_k^{cv}, I_4),\ F_k^{cv} = \mathrm{diag}(F, F),\ F = \begin{bmatrix} 1 & T \\ 0 & 1 \end{bmatrix}$$

$$G_k = \mathrm{diag}(G_k^{cv}, I_4),\ G_k^{cv} = \mathrm{diag}(G, G),\ G = \begin{bmatrix} \frac{T^2}{2} \\ T \end{bmatrix}$$

$$Q = \mathrm{diag}(\tilde{Q}, Q^s),\ \tilde{Q} = 0.1 \cdot I_2,\ Q^s = 0.1 \cdot I_4$$

$$w_{k-1} \sim N(0, Q),\ v_k^r \sim N(0, R),\ R = 0.1^2 \cdot I_2$$

where I_n is the $n \times n$ identity matrix and these parameters were used in the state evolution model $x_k = F_k x_{k-1} + G_k w_{k-1}$ and the measurement model $z_k^r = g(x_k, v_k^r)$. Generally, the number of measurements depends on the size of the extended object, its distance from the radar, the resolution of radars, etc. In our simulation, at each time the automotive radar emitted 180 lines, which divided 2π into 180 equal parts. The detected points were the positions where these lines hit the object, as shown in Fig. 2. The initial estimated extension was set as a square with sides of length 1.

In the simulation, a rectangular object 4m long and 1.6m wide moves at nearly constant-velocity (CV). A vehicle equipped with radar moves along the trajectory represented by the green stars shown in Fig. 4(a). It follows the object on the left at the beginning of the tracking. After several time steps, the vehicle (radar) takes a turn and follows the object on the right.

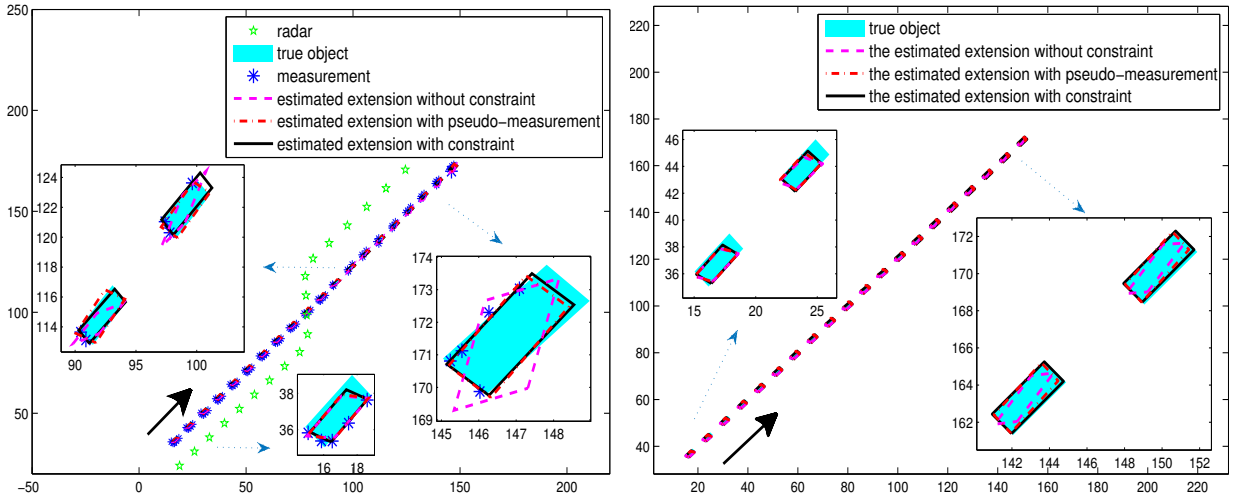

(a) Estimation results in one Monte Carlo run

(b) Average results (over 100 Monte Carlo runs)

Figure 4: Estimation results of the proposed approaches

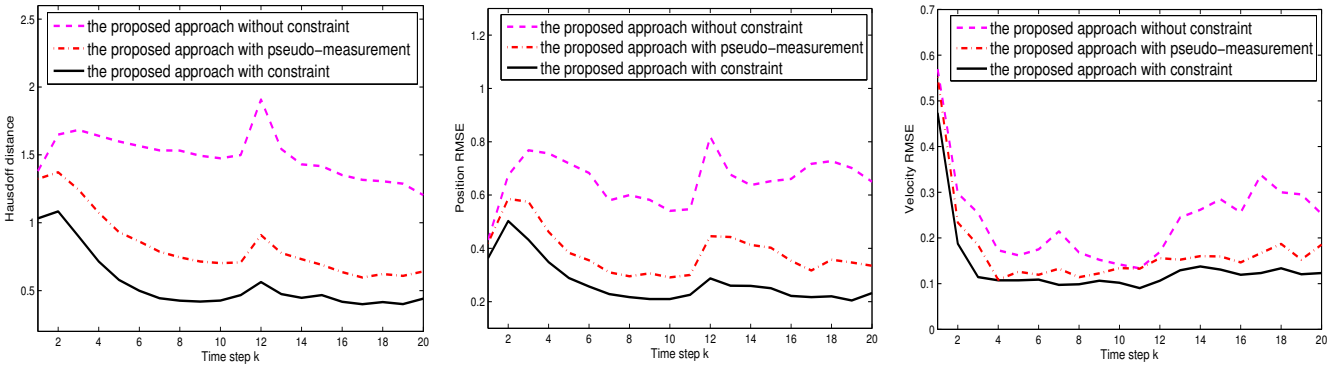

(a) Hausdorff distance

(b) Position RMSE

(c) Velocity RMSE

Figure 5: Performance evaluation of the proposed approaches (averaged over 100 Monte Carlo runs)

Three approaches are compared: the proposed approach without the constraint, the one with pseudo-observations, and the one with the constraint (using both the pseudo-observation and the projection methods).

We choose the root-mean-squared error (RMSE) and the Hausdorff distance as measures for evaluating the tracking performance of the kinematic state and that of the extension estimation, respectively. A specific form to calculate the Hausdorff distance is given by equation (1) in [28]. The Hausdorff distance at time k is calculated with the vertices of the estimated extension and of the true one.

Simulation results in this scenario are shown in Fig. 4. Fig. 4(a) shows the results in a typical Monte Carlo run, where we can also see the measurements at each time. The average estimation results in the same scenario over 100 Monte Carlo runs are presented in Fig. 4(b).

As shown in Fig. 4, in the first several time steps, the estimated shapes using the three approaches are all quite different from the true object. As more measurements are available, the estimated shapes become more and more similar to the true one. Fig. 4(a) also shows that when the radar makes a turn and the measurement configuration is changed, the performance provided by the proposed approach is still good, which illustrates its effectiveness.

Comparison results in terms of the Hausdorff distance and RMSE are presented in Figs. 5(a)–(c). From the three subfigures we can see that the estimation errors are large in the first several time steps. As more measurements are used, the errors drop gradually. As the radar takes a turn at the 11th step, the estimation errors increase, which is caused by the change of the measurement configuration.

Figs. 5(a)–(c) also show that the approach considering the constraint (using both pseudo-observation and projection) provides the best estimation performance of the kinematic state and extension. The approach with pseudo-observation outperforms the one without the constraint, demonstrating the benefit of pseudo-observation. The above illustrates the effectiveness of incorporating the shape constraint information

into EOT.

Computational complexity of the three approaches is also compared. The average computation time for one run (20 steps) of the approach without constraints, the one with pseudo-observation, and the one considering the constraint are 0.3974, 0.3977, and 0.4002 seconds, respectively. That is, the computational complexities of the three approaches are close to one another.

In general, simulation results illustrate the effectiveness of the proposed approach.

IV. Conclusion

Tracking of extended objects using automotive radars is of practical importance. In this paper, a novel and handy model for EOT using automotive radar measurements is introduced. Prior information that the object is rectangular is used in the model as a quadratic equality constraint on the state. Based on this model, an estimation approach is proposed to track extended objects using automotive radars.

Using the special features of tracking rectangular objects, the data association in the approach is largely simplified. The approach also incorporates both pseudo-observation and projection methods, so the shape constraint can be adequately utilized to improve estimation performance. Simulation results for EOT demonstrate the effectiveness of the proposed modeling and estimation.

The proposed approach provides a simple yet effective framework using shape constraints for tracking extended objects with regular shapes, e.g., objects with polygon extensions. The proposed approach can be extended for EOT using multiple automotive radars.

References

[1] Y. Bar-Shalom and X. R. Li, *Estimation and Tracking: principles, techniques, and software*. Boston, MA: Artech House, 1993. (Reprinted by YBS Publishing, 1998).

[2] M. J. Waxman and O. E. Drummond, "A Bibliography of Cluster (Group) Tracking," in *Proceedings of the SPIE Conference on Signal and Data Processing of Small Targets*, Orlando, Florida, USA, Apr. 2004, pp. 551–560.

[3] P. Brobeit, M. Rapp, N. Appenrodt, and J. Dickmann, "Probabilistic Rectangular-Shape Estimation for Extended Object Tracking," in *Proceedings of the IEEE Intelligent Vehicles Symposium (IV)*, Gothenburg, Sweden, Jun. 2016.

[4] B. Kim, K. Yi, H. Yoo, H. Chong, and B. Ko, "An IMM/EKF Approach for Enhanced Multitarget State Estimation for Application to Integrated Risk Management System," *IEEE Transactions on Vehicular Technology*, vol. 64, no. 3, March 2015.

[5] C. Knill, A. Scheel, and K. Dietmayer, "A Direct Scattering Model for Tracking Vehicles with High-Resolution Radars," in *Proceedings of the 2016 IEEE Intelligent Vehicles Symposium*, Gothenburg, Sweden, June 2016, pp. 298–303.

[6] F. E. Daum and R. J. Fitzgerald, "Importance of Resolution in Multiple-Target Tracking," in *Proceedings of the SPIE Conference on Signal and Data Processing of Small Targets*, Orlando, Florida, USA, July 1994, pp. 329–338.

[7] X. R. Li and J. Dezert, "Layered Multiple-Model Algorithm with Application to Tracking Maneuvering and Bending Extended Target in Clutter," in *Proceedings of the 1st International Conference on Information Fusion*, Las Vegas, NV, USA, July 1998, pp. 207–214.

[8] B. -T. Vo, B. -N. Vo, and A. Cantoni, "Bayesian Filtering with Random Finite Set Observations," *IEEE Transactions on Signal Processing*, vol. 56, no. 4, pp. 1313–1326, 2008.

[9] W. Koch and G. van. Keuk, "Multiple Hypothesis Track Maintenance with Possibly Unresolved Measurements," *IEEE Transactions on Aerospace and Electronic Systems*, vol. 33, no. 3, pp. 883–892, 1997.

[10] K. Gilholm, S. Godsill, S. Maskell, and D. Salmond, "Poisson Models for Extended Target and Group Tracking," in *Proceedings of the SPIE Conference on Signal and Data Processing of Small Targets*, San Diego, USA, Sep. 2005, vol. 5913, pp. 230–241.

[11] J. W. Koch, "Bayesian Approach to Extended Object and Cluster Tracking Using Random Matrices," *IEEE Transactions on Aerospace and Electronic Systems*, vol. 44, no. 3, pp. 1042–1059, 2008.

[12] M. Feldmann, D. Franken, and W. Koch, "Tracking of Extended Objects and Group Targets Using Random Matrices," *IEEE Transactions on Signal Processing*, vol. 59, no. 4, pp. 1409–1420, 2011.

[13] J. Lan and X. R. Li, "Tracking of Extended Object or Target Group Using Random Matrix: New Model and Approach," *IEEE Transactions on Aerospace and Electronic Systems*, vol. 52, no. 6, pp. 2973–2989, 2016.

[14] J. Lan and X. R. Li, "Tracking of Maneuvering Non-Ellipsoidal Extended Object or Target Group Using Random Matrix," *IEEE Transactions on Signal Processing*, vol. 62, no. 9, pp. 2450–2463, 2014.

[15] M. Baum, B. Noack, and U. D. Hanebeck, "Extended Object and Group Tracking with Elliptic Random Hypersurface Models," in *Proceedings of the 13th International Conference on Information Fusion (Fusion 2010)*, Edinburgh, United Kingdom, 2010.

[16] M. Baum and U. D. Hanebeck, "Shape Tracking of Extended Objects and Group Targets with Star-Convex RHMs," in *Proceedings of the 14th International Conference on Information Fusion (Fusion 2011)*, Chicago, Illinois, USA, 2011.

[17] A. Zea, F. Faion, M. Baum, U. D. Hanebeck, "Level-Set Random Hypersurface Models for Tracking Nonconvex Extended Objects," *IEEE Transactions on Aerospace and Electronic Systems*, vol. 52, no. 6, pp. 2990–3007, 2016.

[18] C. Adam, R. Schubert, and G. Wanielik, "Radar-Based Extended Object Tracking Under Clutter using Generalized Probabilistic Data Association," in *Proceedings of the 16th International IEEE Annual Conference on Intelligent Transportation Systems*, The Hague, The Netherlands, October, 2013.

[19] A. Scheel and K. Dietmayer, "Tracking Multiple Vehicles using a Variational Radar Model," arXiv preprint arXiv:1711.03799.

[20] Y. Bar-Shalom and X. R. Li, *Multitarget-Multisensor Tracking: Principles and Techniques*. Storrs, CT: YBS Publishing, 1995.

[21] R. J. Hewett, M. T. Heath, M. D. Butala, and F. Kamalabadi, "A Robust Null Space Method for Linear Equality Constrained State Estimation," *IEEE Transactions on Signal Processing*, vol. 58, no. 8, pp. 3961–3971, 2010.

[22] L. Markley, "Attitude Error Representations for Kalman Filter," *Journal of Guidance, Control, and Dynamics*, vol. 26, no. 2, pp. 311–317, 2003.

[23] M. Tahk and J. L. Speyer, "Target Tracking Problems Subject to Kinematic Constraints," *IEEE Transactions on Automatic Control*, vol. 35, no. 3, pp. 324–326, 1990.

[24] A. T. Alouani and W. D. Blair, "Use of a Kinematic Constraint in Tracking Constant Speed, Maneuvering Targets," *IEEE Transactions on Automatic Control*, vol. 38, no. 7, pp. 1107–1111, 1993.

[25] D. Simon and T. L. Chia, "Kalman Filter with State Equality Constraints," *IEEE Transactions on Aerospace and Electronic Systems*, vol. 38, no. 1, pp. 128–136, 2002.

[26] C. Yang and E. Blasch, "Kalman Filtering with Nonlinear State Constraints," in *Proceedings of the 9th International Conference on Information Fusion (Fusion 2006)*, Florence, Italy, 2006.

[27] X. R. Li and V. P. Jilkov, "Survey of Maneuvering Target Tracking–Part I: Dynamic models," *IEEE Transactions on Aerospace and Electronic Systems*, vol. 39, no. 4, pp. 1333–1364, 2003

[28] D. Schuhmacher, B. -T. Vo, and B. -N. Vo, "A Consistent Metric for Performance Evaluation of Multi-Object Filters," *IEEE Transactions on Signal Processing*, vol. 56, no. 8, pp. 3447–3457, 2008.